

Exploring Complex Phases of the MSSM at Future Colliders

S. Heinemeyer

CERN TH Division, Department of Physics, CH-1211 Geneva 23, Switzerland

M. Velasco

Northwestern University, Evanston, Illinois 60201, USA

Once Supersymmetry is discovered, exploring the phases of supersymmetric parameters will be one of the most important tasks of future colliders. We analyze the possibilities of investigating the phases of the cMSSM via their effects on the Higgs sector through radiative corrections. Within two benchmark scenarios we compare the capabilities of the LHC, the ILC and a future γC .

1. INTRODUCTION

The Minimal Supersymmetric Standard Model (cMSSM) may possess several complex phases. These phases can enter via loop corrections into the Higgs boson sector [1] and affect the Higgs boson masses and couplings [2, 3, 4, 5, 6, 7]. Most prominently the phase of the third generation trilinear couplings, $\phi_{A_{t,b}}$, have an effect, while the phases from the gaugino sector usually have a smaller impact. At the two-loop level also the phase of the gluino, $\phi_{\tilde{g}}$, can enter. Measuring these phases will be one of the important tasks of future high-energy colliders.

We discuss the impact of complex phases within the MSSM on various Higgs boson production and decay channels. Results are compared for a the LHC, the ILC, and a $\gamma\gamma$ collider (γC). While the precision of the branching ratio measurement at the LHC is not accurate enough, both the ILC and the γC could in principle be sensitive to the effects of complex phases (depending on the scenario). The precisions for the various Higgs boson decay channels at the three colliders are summarized in tab. I. The Higgs boson mass is set to “typical” values below the upper bound of $m_h \lesssim 140$ GeV [8, 9], which is valid in the real as well as in the complex MSSM.

Table I: Expected experimental precision of the rate measurement of $h \rightarrow X$ at the LHC, the ILC operating at $\sqrt{s} = 500, 1000$ GeV, and the γC (based on the CLICHE design [10]).

Study	m_h	$b\bar{b}$	WW^*	$\tau^+\tau^-$	$c\bar{c}$	gg	$\gamma\gamma$
LHC [11]	120 GeV	$\sim 20\%$	$\sim 10\%$	$\sim 15\%$	—	—	—
ILC ($\sqrt{s} = 500$ GeV) [12, 13]	120 GeV	1.5%	3%	4.5%	6%	4%	19%
ILC ($\sqrt{s} = 1000$ GeV) [12, 14]	120 GeV	1.5%	2%	—	—	2.3%	5.4%
γC [10, 15]	115 GeV	2%	5%	—	—	—	22%

2. COMPARISON OF DIFFERENT COLLIDERS

We compare the sensitivity of a future γC with that of the LHC and the ILC. The comparison is based on two different physics scenarios:

The CPX scenario:

This scenario has been designed to give maximum effects of CP-violating phases [16]. The parameters are

$$\begin{aligned} M_{\text{SUSY}} &= 500 \text{ GeV}, |A_t| = 1000 \text{ GeV}, A_t = A_b = A_\tau \\ M_2 &= 500 \text{ GeV}, |m_{\tilde{g}}| = 1000 \text{ GeV}, \mu = 2000 \text{ GeV} \\ \phi &= \phi_{A_{t,b,\tau}} = \phi_{m_{\tilde{g}}} \end{aligned} \quad (1)$$

M_{SUSY} denotes a common soft SUSY-breaking mass in the sfermion mass matrices. A_f is the trilinear Higgs-Sfermion coupling with the phase ϕ_f . M_2 is a gaugino mass parameter, $m_{\tilde{g}}$ denotes the gluino mass, and μ is the Higgs mixing parameter.

The BGX scenario:

This scenario is motivated by baryogenesis. It has been shown in [17] that in this scenario (depending on the Higgs sector parameters) baryogenesis in the early universe could be possible. It is thus a physics motivated scenario, not emphasising possible effects of complex phases. The parameters are

$$\begin{aligned} M_{\tilde{t}_{L,R}} &= 1.5 \text{ TeV}, M_{\tilde{t}_R} = 0, M_{\tilde{Q}_{1,2}} = 1.2 \text{ TeV}, M_{\tilde{L}_{1,2}} = 1.0 \text{ TeV} \\ |X_t| &= 0.7 \text{ TeV}, A_t = A_b = A_\tau \\ M_2 &= 220 \text{ GeV}, m_{\tilde{g}} = 1 \text{ TeV}, \mu = 200 \text{ GeV} \\ \phi &= \phi_{A_{t,b,\tau}} = \phi_{m_{\tilde{g}}} \end{aligned} \quad (2)$$

Here $M_{\tilde{t}_{L,R}}$ are the soft SUSY-breaking parameters in the scalar top mass matrix. $M_{\tilde{Q}_{1,2}}$ are the corresponding parameters for the squarks of the first two generations, while $M_{\tilde{L}_{1,2}}$ refer to the sleptons of the first two generations. $m_t X_t$ is the off-diagonal entry in the scalar top mass matrix with $X_t = A_t - \mu/\tan\beta$.

The results presented here have been obtained with the code *FeynHiggs2.2* [6, 8, 9, 18]. It should be noted that the higher-order uncertainties in these evaluations are somewhat less under control as compared to the real case, see e.g. Ref. [19]. The same applies to the parametric uncertainties due to the experimental errors of the input parameters [19, 20, 21, 22]. Results for branching ratios obtained with an alternative code, *CPsuperH* [23], can differ quantitatively to some extent from the results shown here. A main difference between the two codes are the more complete inclusion of real two-loop corrections in *FeynHiggs2.2*, resulting in somewhat higher values for the lightest Higgs boson mass. While the complex phase dependence at the one-loop level is included completely in *FeynHiggs2.2*, at the two-loop level it is more complete in *CPsuperH*, which makes it difficult to disentangle the source of possible deviations. A more complete discussion can be found in [24].

2.1. The CPX scenario

We start our analysis by the investigation of the CPX scenario, see eq. 1. We first show the results for the γC in fig. 1 for the decay channel $h \rightarrow b\bar{b}$, which has the best sensitivity at this collider. The variation of $\Gamma_{\gamma\gamma} \times \text{BR}(h \rightarrow b\bar{b})$ is shown in the $\phi_{A_{t,b}} - \tan\beta$ plane. The strips correspond to constant values of the lightest Higgs mass, while the color code shows the deviation from the corresponding SM value. It should be kept in mind that the Higgs boson mass will be measured to very high accuracy so that one will be confined to one of the strips. We are neglecting the parametric errors from the imperfect knowledge of the input parameters. In reality these parametric errors would widen the strips. The future intrinsic error of $\sim 0.5 \text{ GeV}$ [20], however, is included in the width of the strips. One can see that this channel can be strongly enhanced as compared to the SM. The variation along each strip is much larger than the anticipated precision of $\sim 2\%$ for this channel. This would allow to constrain the values of the complex phases. The picture becomes of course more complicated if the complex phases are varied independently. Various channels will have to be combined to disentangle the different effects.

Results for the LHC are shown in fig. 2. The left plots gives the results for the channel $gg \rightarrow h \rightarrow \gamma\gamma$, while the right plots depicts $WW \rightarrow h \rightarrow \tau^+\tau^-$. The latter channel (like $h \rightarrow b\bar{b}$) is usually somewhat enhanced in the MSSM,

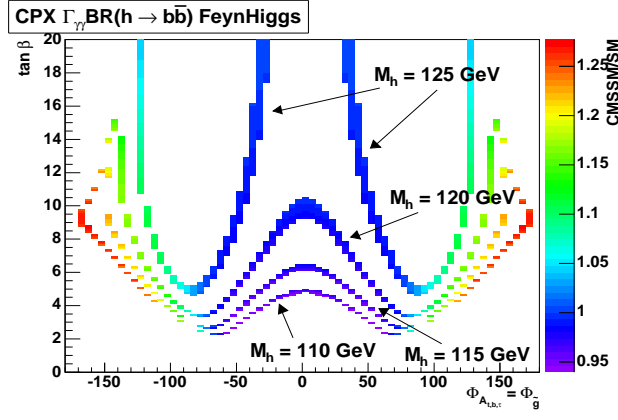


Figure 1: The deviations of $\Gamma_{\gamma\gamma} \times \text{BR}(h \rightarrow b\bar{b})$ within the CPX scenario from the SM value is shown in the $\phi_{A_{t,b}} - \tan\beta$ plane. The corresponding precision obtainable at a γC is $\sim 2\%$.

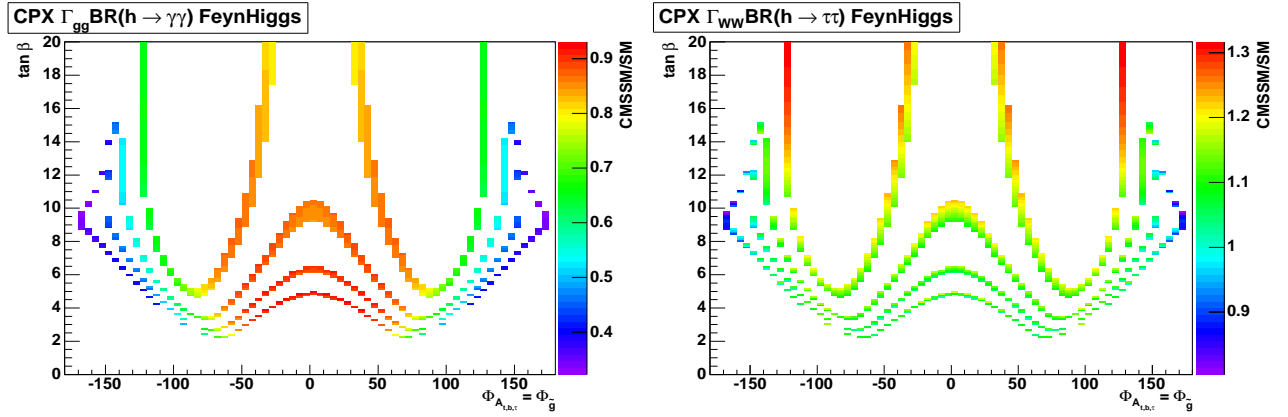


Figure 2: The deviations of $\Gamma_{gg} \times \text{BR}(h \rightarrow \gamma\gamma)$ (left) and of $\Gamma_{WW} \times \text{BR}(h \rightarrow \tau^+\tau^-)$ (right) within the CPX scenario from the SM value is shown in the $\phi_{A_{t,b}} - \tan\beta$ plane. The corresponding experimental precision can be found in tab. I.

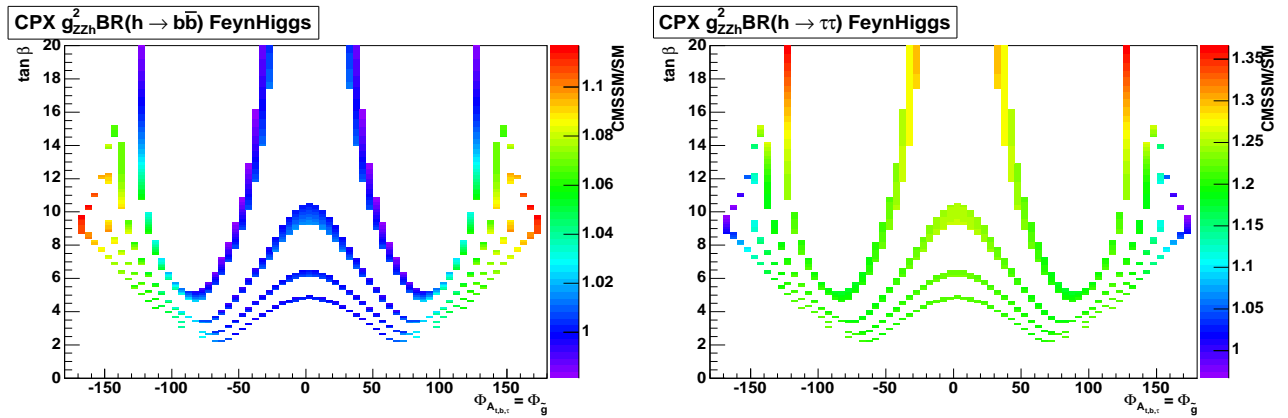


Figure 3: The deviations of $g_{ZZh}^2 \times \text{BR}(h \rightarrow b\bar{b})$ (left) and of $g_{ZZh}^2 \times \text{BR}(h \rightarrow \tau^+\tau^-)$ (right) within the CPX scenario from the SM value is shown in the $\phi_{A_{t,b}} - \tan\beta$ plane. The corresponding experimental precision can be found in tab. I.

the $\text{BR}(h \rightarrow WW^*)$ (not shown) and $\text{BR}(h \rightarrow \gamma\gamma)$ (see the left plot of 2) are normally suppressed in this scenario. The precision of the LHC will not be good enough to obtain information about complex phases in this way.

Finally in fig. 3 shows the ILC results in the CPX scenario. The left plot shows the $\text{BR}(h \rightarrow b\bar{b})$, while the right plot depicts $\text{BR}(h \rightarrow \tau^+\tau^-)$. Both channels are enhanced as compared to the SM in this scenario. The high precision of the ILC (see I) shows that this collider has a good potential to disentangle the complex phases.

Since in the examples shown here for the γC and the ILC the largest deviations occur for different regions of the parameter space, the results from both colliders could be combined in order to extract the maximum information on $\phi_{A_{t,b}}$.

2.2. The BGX scenario

Now we turn to the investigation of the baryogenesis motivated BGX scenario, see eq. 2. The effects in this scenario are expected to be smaller than in the CPX scenario that had been designed to give maximum effects of the complex phases.

In fig. 4 we show the $h \rightarrow b\bar{b}$ channel at the γC . A substantial suppression with respect to the SM can be observed. However, the variation of $\Gamma_{\gamma\gamma} \times \text{BR}(h \rightarrow b\bar{b})$ for fixed Higgs boson mass (which will be known with high precision) with the complex phase $\phi_{A_{t,b}}$ is very small. Thus a precise measurement of this channel at the γC will not reveal any information about the complex phases entering the MSSM Higgs sector.

The two LHC channels in the BGX scenario are shown in fig. 5, while the two ILC channels are given in fig. 6. As for the CPX scenario no phase measurement can be expected from the LHC measurements. The situation at the ILC in the BGX scenario is similar to the γC . A deviation from the SM value can be measured, but the variation of $g_{ZZh}^2 \times \text{BR}(h \rightarrow b\bar{b}, \tau^+\tau^-)$ is too small to reveal any information on $\phi_{A_{t,b}}$.

3. CONCLUSIONS

We have compared the LHC, the ILC and the γC in view of their power to determine the complex phases of the cMSSM. We have focused on the Higgs sector, where the complex phases enter via radiative corrections. Especially we have investigated the most promising combinations of Higgs production and decay ($\sigma \times \text{BR}$) for each collider.

The analysis has been performed in two scenarios: The CPX scenario designed to maximize the effect of complex phases in the MSSM Higgs sector. The other scenario (BGX) is based on a part of the cMSSM that is motivated by baryogenesis.

The CPX scenario may offer good prospects for the γC and the ILC to determine $\phi_{A_{t,b}}$ via Higgs branching ratio measurements. On the other hand, the BGX scenario will only show a deviation from the SM. The variation of the analyzed channels is too small to give information on the complex phases.

It should be kept in mind that we have neglected the future parametric errors on the SUSY parameters (see e.g. Ref. [25] and references therein). These uncertainties will further widen the bands shown in figs. 1–6.

Acknowledgments

S.H. thanks C. Wagner for helpful discussions concerning the BGX scenario.

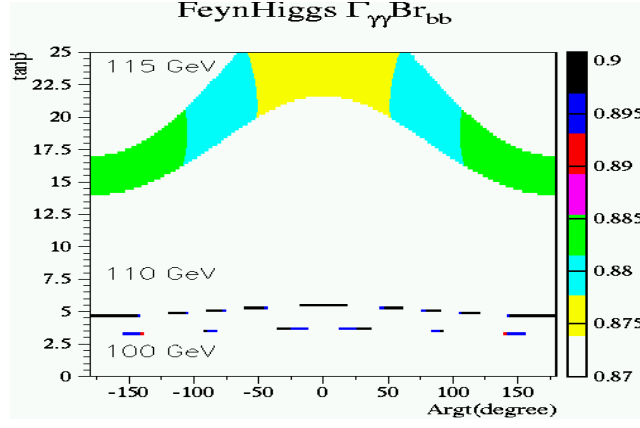


Figure 4: The deviations of $\Gamma_{\gamma\gamma} \times \text{BR}(h \rightarrow b\bar{b})$ within the BGX scenario from the SM value is shown in the $\phi_{A_{t,b}} - \tan\beta$ plane. The corresponding precision obtainable at a γC is $\sim 2\%$.

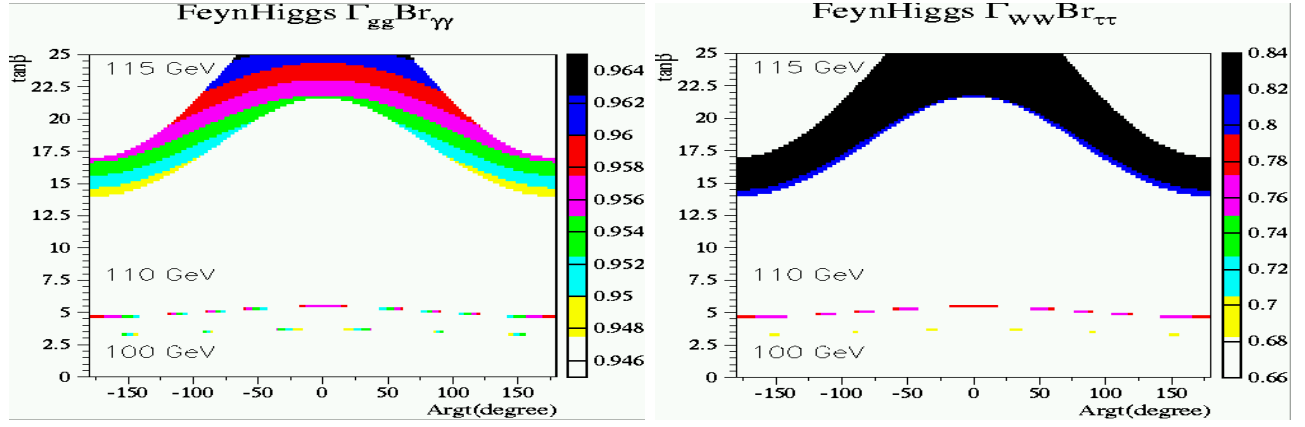


Figure 5: The deviations of $\Gamma_{gg} \times \text{BR}(h \rightarrow \gamma\gamma)$ (left) and of $\Gamma_{WW} \times \text{BR}(h \rightarrow \tau^+\tau^-)$ (right) within the BGX scenario from the SM value is shown in the $\phi_{A_{t,b}} - \tan\beta$ plane. The corresponding experimental precision can be found in tab. I.

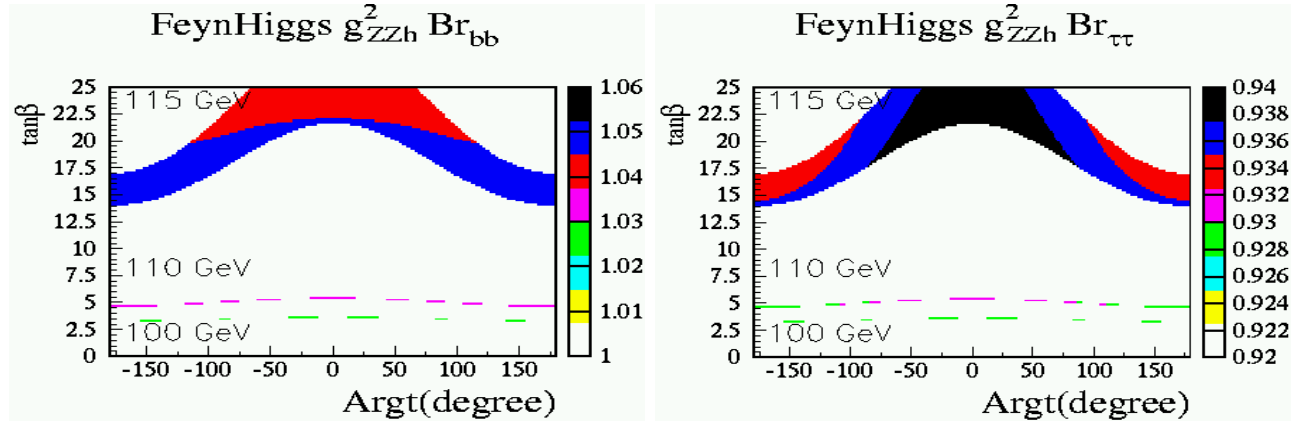


Figure 6: The deviations of $g_{ZZh}^2 \times \text{BR}(h \rightarrow b\bar{b})$ (left) and of $g_{ZZh}^2 \times \text{BR}(h \rightarrow \tau^+\tau^-)$ (right) within the BGX scenario from the SM value is shown in the $\phi_{A_{t,b}} - \tan\beta$ plane. The corresponding experimental precision can be found in tab. I.

References

- [1] A. Pilaftsis, *Phys. Rev. D* **58** (1998) 096010, hep-ph/9803297;
A. Pilaftsis, *Phys. Lett. B* **435** (1998) 88, hep-ph/9805373.
- [2] D. Demir, *Phys. Rev. D* **60** (1999) 055006, hep-ph/9901389;
S. Choi, M. Drees and J. Lee, *Phys. Lett. B* **481** (2000) 57, hep-ph/0002287.
- [3] A. Pilaftsis and C. Wagner, *Nucl. Phys. B* **553** (1999) 3, hep-ph/9902371.
- [4] M. Carena, J. Ellis, A. Pilaftsis and C. Wagner, *Nucl. Phys. B* **586** (2000) 92, hep-ph/0003180.
- [5] T. Ibrahim and P. Nath, *Phys. Rev. D* **63** (2001) 035009, hep-ph/0008237; *Phys. Rev. D* **66** (2002) 015005, hep-ph/0204092.
- [6] S. Heinemeyer, *Eur. Phys. Jour. C* **22** (2001) 521, hep-ph/0108059.
- [7] M. Frank, S. Heinemeyer, W. Hollik and G. Weiglein, hep-ph/0212037, appeared in the proceedings of SUSY02, DESY, Hamburg, Germany, July 2002.
- [8] S. Heinemeyer, W. Hollik and G. Weiglein, *Eur. Phys. Jour. C* **9** (1999) 343, hep-ph/9812472.
- [9] G. Degrandi, S. Heinemeyer, W. Hollik, P. Slavich and G. Weiglein, *Eur. Phys. Jour. C* **28** (2003) 133, hep-ph/0212020.
- [10] D. Asner, H. Burkhardt, A. De Roeck, J. Ellis, J. Gronberg, S. Heinemeyer, M. Schmitt, D. Schulte, M. Velasco and F. Zimmermann, *Eur. Phys. Jour. C* **28** (2003) 27, hep-ex/0111056.
- [11] M. Dührssen, S. Heinemeyer, H. Logan, D. Rainwater, G. Weiglein and D. Zeppenfeld, *Phys. Rev. D* **70** (2004) 113009, hep-ph/0406323; hep-ph/0407190.
- [12] J. Aguilar-Saavedra et al., TESLA TDR Part 3, hep-ph/0106315, see: tesla.desy.de/tdr.
- [13] J. Brient, talk at the LCWS, Cracow, Poland, September 2001,
see: webnt.physics.ox.ac.uk/lc/ecfadesy
- [14] T. Barklow, hep-ph/0312268.
- [15] D. Asner et al., hep-ph/0308103.
- [16] M. Carena, J. Ellis, A. Pilaftsis, C. Wagner, *Phys. Lett. B* **495** (2000) 155, hep-ph/0009212.
- [17] C. Balazs, M. Carena, A. Menon, D. E. Morrissey and C. E. M. Wagner, hep-ph/0412264.
- [18] S. Heinemeyer, W. Hollik, G. Weiglein, *Comp. Phys. Comm.* **124** (2000) 76, hep-ph/9812320;
M. Frank, T. Hahn, S. Heinemeyer, W. Hollik, G. Weiglein, *in preparation*.
The code can be obtained from www.feynhiggs.de.
- [19] S. Heinemeyer, hep-ph/0407244.
- [20] S. Heinemeyer, W. Hollik and G. Weiglein, hep-ph/0412214.
- [21] S. Heinemeyer, W. Hollik and G. Weiglein, *JHEP* **0006** (2000) 009, hep-ph/9909540.
- [22] B. Allanach, A. Djouadi, J. Kneur, W. Porod and P. Slavich, *JHEP* **0409** (2004) 044, hep-ph/0406166.
- [23] J. Lee, A. Pilaftsis et al., *Comp. Phys. Comm.* **156** (2004) 283, hep-ph/0307377.
- [24] S. Heinemeyer, W. Hollik, H. Rzehak and G. Weiglein, *preparation*.
- [25] G. Weiglein et al. [LHC / ILC Study Group], hep-ph/0410364.